THE JOURNAL OF BIOLOGICAL CHEMISTRY VOL. 287, NO. 37, pp. 31561–31573, September 7, 2012


# A Substrate Binding Hinge Domain Is Critical for Transport-related Structural Changes of Organic Cation Transporter 1*[S]

Received for publication, June 6, 2012, and in revised form, July 16, 2012 Published, JBC Papers in Press, July 18, 2012, DOI 10.1074/jbc.M112.388793

**Brigitte Egenberger[‡], Valentin Gorboulev[‡], Thorsten Keller[‡], Dmitry Gorbunov[‡], Neha Gottlieb[‡], Dietmar Geiger[§], Thomas D. Mueller[§], and Hermann Koepsell[‡1]**

*From the [‡]Institute of Anatomy and Cell Biology, University of Würzburg, 97070 Würzburg and the [§]Department of Molecular Plant Physiology and Biophysics, Julius-von-Sachs-Institute, University of Würzburg, 97082 Würzburg, Germany*

**Background:** The transport mechanism of organic cation transporter OCT1 is not understood.
**Results:** Voltage-dependent movements of transmembrane $\alpha$-helices in OCT1 were identified that were blocked by mutations of glycine in the substrate binding domain of $\alpha$-helix 11.
**Conclusion:** A hinge domain pivotal for transport-related structural changes has been identified.
**Significance:** The hinge domain allows substrate occlusion during translocation.

**Organic cation transporters are membrane potential-dependent facilitative diffusion systems. Functional studies, extensive mutagenesis, and homology modeling indicate the following mechanism. A transporter conformation with a large outward-open cleft binds extracellular substrate, passes a state in which the substrate is occluded, turns to a conformation with an inward-open cleft, releases substrate, and subsequently turns back to the outward-open state. In the rat organic cation transporter (rOct1), voltage- and ligand-dependent movements of fluorescence-labeled cysteines were measured by voltage clamp fluorometry. For fluorescence detection, cysteine residues were introduced in extracellular parts of cleft-forming transmembrane $\alpha$-helices (TMHs) 5, 8, and 11. Following expression of the mutants in *Xenopus laevis* oocytes, cysteines were labeled with tetramethylrhodamine-6-maleimide, and voltage-dependent conformational changes were monitored by voltage clamp fluorometry. One cysteine was introduced in the central domain of TMH 11 replacing glycine 478. This domain contains two amino acids that are involved in substrate binding and two glycine residues (Gly-477 and Gly-478) allowing for helix bending. Cys-478 could be modified with the transported substrate analog [2-(trimethylammonium)-ethyl]methanethiosulfonate but was inaccessible to tetramethylrhodamine-6-maleimide. Voltage-dependent movements at the indicator positions of TMHs 5, 8, and 11 were altered by substrate applications indicating large conformational changes during transport. The G478C exchange decreased transporter turnover and blocked voltage-dependent movements of TMHs 5 and 11. [2-(Trimethylammonium)-ethyl]methanethiosulfonate modification of Cys-478 blocked substrate binding, transport activity, and movement of TMH 8. The data suggest that Gly-478 is located within a mechanistically important hinge domain of TMH 11 in which substrate binding induces transport-related structural changes.**

Polyspecific organic cation transporters (OCTs)[2] of the SLC22 transporter family play a pivotal role in absorption, excretion, and tissue distribution of drugs and endogenous compounds, including neurotransmitters (1). Polymorphisms that change expression level, regulation, turnover, and/or substrate affinity of these transporters can potentially influence therapeutic efficiency and may cause toxic side effects of individual drugs (2). For example, patients with mutations in human organic cation transporter 1 (hOCT1) interfering with its function are poor responders to metformin treatment of type 2 diabetes because the uptake of the antidiabetic drug into hepatocytes is impaired (3). Molecular understanding of ligand recognition by OCTs and of the mechanism(s) how OCTs mediate(s) substrate translocation is of high interest and has a huge potential for biomedical use. The analysis of interaction surfaces of the transporters and different ligands allows a tentative prediction whether and how new ligands interact with the transporters, thus providing a first basis for drug design. For discrimination between transported substrates and nontransported inhibitors, the translocation process must be understood. Substrate translocation involves a series of structural changes, which include an outward-open conformation allowing binding of extracellular substrates, a state during which the substrate is occluded and passive diffusion of inorganic ions is minimized, and an inward-open conformation during which the substrate is released (4–6). Extracellular inhibitors may block transport activity not only via competition or allosteric blunting of substrate binding to the outward-open conformation(s) of the transporter(s), but also by preventing of transport-related conformational changes.

Previous studies on organic cation transporters 1 and 2 from rat (rOct1 and rOct2) showed that OCTs are facilitative diffu-

* This work was supported by the Deutsche Forschungsgemeinschaft Grants SFB 487/A4 and KO 872/6-1.
[S] This article contains supplemental Figs. 1–11 .
[1] To whom correspondence should be addressed. Tel.: 49-931-3182700; Fax: 49-931-3180586; E-mail: Hermann@Koepsell.de.

[2] The abbreviations used are: OCT, organic cation transporter; h, human; r, rat; LacY, lactose permease of *E. coli*; TMH, transmembrane $\alpha$-helix; $TBuA^+$, tetrabutylammonium; $MPP^+$ 1-methyl-4-phenylpyridinium$^+$; $TEA^+$, tetraethylammonium$^+$; $MTSET^+$, [2-(trimethylammonium) ethyl]methanethiosulfonate bromide$^+$; TMRM, tetramethylrhodamine-6-maleimide; D-PBS, Dulbecco's PBS.

sion systems mediating electrogenic cation uniport in both directions across the plasma membrane (7, 8). The substrate concentration gradient and the membrane potential provide the driving force for cation translocation. At membrane potentials between −50 and −100 mV, translocation of organic cations occurs without flux of inorganic ions (9). By employing structural models derived from the structure of the lactose permease of *Escherichia coli* (LacY) in combination with extensive mutagenesis, we identified amino acids in substrate binding regions of both the outward-open and inward-open conformation of rOct1 (4, 10–12). We provided evidence that five amino acids interact with both extracellular and intracellular ligands. In our models, these amino acids are located in the innermost cavities of the outward-open and inward-open clefts of rOct1.

Little is known about structural changes taking place during transition of the outward-open into the inward-open conformation. This structural change is supposed to be initiated by substrate binding to the outward-open conformation. The membrane potential dependence of organic cation transport suggests that the transport-related conformational changes are partially identical to conformational changes that can be induced by changes of the membrane potential. Most probably, such changes are influenced by substrates. For modeling of the outward-open conformation we assumed, in analogy to LacY, that the structural change from the outward-open to the inward-open conformations involves a rigid body movement of the six N-terminal transmembrane $\alpha$-helices (TMHs) against the six C-terminal TMHs (13). The validity of the outward-open cleft model was supported by mutagenesis experiments indicating that amino acids lining the predicted outward-open cleft are critical for interaction of the extracellular nontransported inhibitors tetrabutylammonium$^+$ ($TBuA^+$) and corticosterone with the transporter (12). The models suggest that the cleft-forming TMHs are straight with the exception of TMH 4 that seems slightly bent. However, bending and/or twisting of helices is required to form the proposed intermediate state in which the substrate is occluded. Employing voltage clamp fluorometry, membrane potential-dependent and ligand-induced movements of two amino acids in TMH 11 close to the extracellular surface of the plasma membrane (Phe-483 and Phe-486) were demonstrated (13). It remained unclear whether the movements of these amino acids represent local changes of TMH 11 because of substrate binding to this TMH (14) or whether the movements are part of a major structural change within the transporter.

In this study, we demonstrate membrane potential-dependent and ligand-induced movements of amino acids in the TMHs 5, 8, and 11 indicating that transport-related structural changes of rOct1 include a minimum of three TMHs. We present evidence for an important mechanistic role of amino acids 474–478 (Cys-Asp-Leu-Gly-Gly) in the middle of TMH 11. Whereas Cys-474 and Asp-475 are involved in binding of $TEA^+$ (14, 15), bending of TMH 11 at Gly-477 and/or Gly-478 (16) is supposed to be important for transport-related structural changes. After replacement of glycine 478 by cysteine or serine, the turnover for MPP uptake slowed down, and membrane potential-dependent movements of TMHs 5 and 11 were blocked.

## EXPERIMENTAL PROCEDURES

*Materials*—[$^3$H]1-Methyl-4-phenylpyridinium$^+$ ($MPP^+$) (3.1 TBq/mmol), [$^{14}$C]tetraethylammonium$^+$ ($TEA^+$) (1.9 GBq/mmol), and [$^{14}$C][2-(trimethylammonium) ethyl] methanethiosulfonate bromide$^+$ ($MTSET^+$) (3.9 GBq/mmol) were obtained from American Radiolabeled Chemicals (St. Louis, MO) and Toronto Research Chemicals Inc. (North York, Canada), respectively. Tetramethylrhodamine-6-maleimide (TMRM) was purchased from Invitrogen, and $MTSET^+$ was from Toronto Research Chemicals Inc. (North York, Canada). All other chemicals were obtained as described earlier (17).

*Constructs for Expression of rOct1 Mutants*—Mutants were generated based on rOct1 or the mutant rOct1(10ΔC) in which 10 cysteine residues were replaced by other amino acids (13, 18). Single point mutations were introduced by polymerase chain reaction applying the overlap extension method (19). The mutations were verified by DNA sequencing. Rat Oct1 (rOct1) and rOct1(G478C) variants with FLAG epitopes at the C termini were generated as described (20). For expression in oocytes, the mutants were cloned into the vector pRSSP (21). For expression of rOct1(10ΔC) and rOct1(10ΔC,G478C) in human embryonic kidney (HEK) 293 cells, rOct1(10ΔC) and rOct1(10ΔC,G478C) were recloned into EcoRV/NotI sites of the vector pcDNA3.1.

*Expression of rOCT1 Mutants in Oocytes*—Purified pRSSP plasmids were linearized with MluI. m7G(5′)ppp(5′)G-capped cRNAs were prepared using the mMESSAGE mMACHINE SP6 kit (Ambion, Huntingdon, UK). The cRNA concentrations were estimated from ethidium bromide-stained agarose gels using polynucleotide markers as standards (22). Stage V–VI *Xenopus laevis* oocytes were obtained by partial ovariectomy, defolliculated with collagenase A, and stored in Ori buffer (5 mM MOPS, 100 mM NaCl, 3 mM KCl, 2 mM $CaCl_2$, 1 mM $MgCl_2$, adjusted to pH 7.4 using NaOH) supplemented with 50 mg/liter gentamicin. The oocytes were injected with 50 nl of $H_2O$/oocyte containing 10 ng of cRNA encoding rOct1 or rOct1 mutants. For transporter expression, the oocytes were incubated 2–5 days at 16 °C in Ori buffer containing 50 mg/liter gentamicin.

*Generation of Stably Transfected HEK293 Cells*—HEK293 cells were stably transfected with rOct1(10ΔC) and rOct1(10ΔC,G478C) and selected as described (23). The cells were cultivated at 37 °C in Dulbecco's modified Eagle's medium containing 3.7 g/liter $NaHCO_3$, 1.0 g/liter D-glucose, 2 mM L-glutamine, 10% heat-inactivated fetal calf serum, 100,000 units/liter penicillin, 100 mg/liter streptomycin, and 0.8 mg/ml geneticin (G418).

*Cysteine Labeling with Fluorescent Dye TMRM*—Fluorescence labeling with the sulfhydryl reagent TMRM was performed with oocytes expressing rOct1(10ΔC) mutants in which one or two amino acids was (were) replaced by cysteine(s). For electrical measurements, five oocytes were incubated for 5 min at room temperature in 0.5 ml of Ori buffer containing 10 $\mu$M TMRM, and the oocytes were washed. Each oocyte contained 4–5 $\mu$g of protein in the plasma membrane (for plasma membrane purification see below). Under this condition, only a fraction of the expressed transporter molecules was labeled; how-

ever, fluorescence due to nonspecifically bound TMRM was minimized. To determine whether TMRM labeling changes transport activity, oocytes expressing the respective mutants were incubated for 5 min (at room temperature) in Ori buffer containing 250 $\mu$M TMRM, and oocytes were subsequently washed at least three times with Ori buffer, and tracer uptake was measured.

*Cysteine Labeling with Substrate Analog MTSET$^+$*—MTSET$^+$ labeling was performed in oocytes and HEK293 cells expressing rOct1(10ΔC) mutants in which one or two individual amino acids was (were) replaced by cysteine(s). For electrical measurements, voltage-clamped oocytes were incubated for 45 s at room temperature in Ori buffer containing different concentrations of MTSET$^+$. For tracer uptake measurements, oocytes (five oocytes in 0.5 ml) were preincubated for 45 s with 50 $\mu$M MTSET$^+$ or for 10 min with 100 $\mu$M MTSET$^+$ at room temperature and then washed at least three times with Ori buffer. For tracer uptake measurements in HEK293 cells, confluent cells were washed with Dulbecco's phosphate-buffered saline (D-PBS), suspended by shaking, collected by 10-min centrifugation at 1,000 × *g*, resuspended for 1 min at 37 °C in D-PBS (at $10^8$ cells/ml) without or with 1 mM MTSET$^+$, and washed three times with D-PBS.

*Two-electrode Voltage Clamp Epifluorescence Measurements*—Measurements were performed in a perfusion chamber that was mounted on the stage of an epifluorescence microscope (Leica DM LFS, Leica Microsystems, Wetzlar, Germany) equipped with a ×40 water immersion objective (24). Membrane currents were measured using the two-electrode voltage clamp amplifier TURBO tec-05X (NPI Electronic GmbH, Tamm, Germany) and the AD/DA converter ITC-16 (Instrutech Corp., Port Washington, NY). Fluorescence was excited by a mercury metal halide lamp (Leica EL6000, Leica Microsystems, Wetzlar, Germany) using a filter system Y3 L (Leica Microsystems, Wetzlar, Germany) (excitation filter 535 nm and emission filter 610 nm). Fluorescence was measured with a PIN-20A photodiode (AMS Technologies AG, München, Germany) and amplified via the low noise current preamplifier model SR570 (Stanford Research Systems, Sunnyvale, CA). Fluorescence and current signals were recorded simultaneously by Patchmaster 2.32 (HEKA, Lambrecht, Germany). Voltage-dependent fluorescence changes ($\Delta F$) were measured after changing the membrane potential from +60 mV to −160 mV in 20-mV steps. The fluorescence changes were normalized according to the equation $\Delta F = (F_V - F_{(-160\ mV)})/F_{(-160\ mV)}$, where $F_{(-160\ mV)}$ represents the fluorescence signal measured at −160 mV. All signals were averaged from 3 to 5 measurements.

*Current and Capacitance Measurements*—Parallel measurements of membrane currents ($I_m$) and membrane capacitance ($C_m$) were performed using a previously described paired ramps approach that allowed us to monitor $C_m$ continuously (25, 26). To determine cation-induced inward currents or cation-induced capacitance changes, the *X. laevis* oocytes were superfused with Ori buffer containing choline$^+$, TEA$^+$, or MPP$^+$.

*Tracer Uptake Measurements in Oocytes*—Oocytes with rOct1 or rOct1 mutants expressed by cRNA injection, and noninjected control oocytes were incubated for 15 or 30 min at room temperature with Ori buffer containing [$^3$H]MPP$^+$, [$^{14}$C]TEA$^+$, or [$^{14}$C]MTSET$^+$ plus different concentrations of nonradioactive substrates and/or inhibitors. Correction for nonspecific uptake was performed by subtracting uptake rates measured in noninjected oocytes from the same batch. After incubation with radioactive compounds, the oocytes were washed three times with ice-cold Ori buffer and solubilized with 5% SDS in water, and the intracellular radioactivity was analyzed by liquid scintillation counting using an LS 6500 counter from Beckman Coulter Inc. (Brea, CA).

*Tracer Uptake Measurements in HEK293 Cells*—Uptake measurements in HEK293 cells were performed at 37 °C. HEK293 cells suspended in D-PBS (at $10^7$ cells/ml) were incubated for 1 s (cells without MTSET$^+$ modification) or 10 s (cells modified with MTSET$^+$) with [$^3$H]MPP$^+$, [$^3$H]MPP$^+$ plus various concentrations of nonradioactive MPP$^+$, or [$^3$H]MPP$^+$ plus various concentrations of tetrabutylammonium$^+$ (TBuA$^+$). Uptake was quenched by addition of ice-cold PBS containing 100 $\mu$M quinine$^+$ (stop solution). Cells were washed three times with ice-cold stop solution, solubilized with 4 M guanidine thiocyanate, and analyzed for radioactivity.

*Tracer Binding Measurements in HEK293 Cells*—Binding measurements in HEK293 cells were performed at 0 °C as described (20). Aliquots of HEK293 cells in D-PBS were transferred to 1.5-ml tubes and incubated for 10 min in ice water. For binding measurements, cells (about $10^7$ cells/ml) were incubated 5 min at 0 °C with 12.5 nM [$^3$H]MPP$^+$ in the absence and presence of 10 nM to 500 $\mu$M nonradioactive MPP$^+$ and in the presence of 5 mM nonradioactive MPP$^+$. After 2 min of centrifugation at 1,000 × *g*, the supernatants were removed carefully. Residual radioactivity on the tube walls was removed by washing with 1 ml of ice-cold D-PBS for 1 s. The pellets were solubilized with 4 M guanidine thiocyanate and analyzed for radioactivity. Nonsaturable [$^3$H]MPP$^+$ binding measured in the presence of 5 mM MPP$^+$ was subtracted from binding measurements performed at lower MPP$^+$ concentrations.

*Preparation of Plasma Membranes from Oocytes*—For one preparation of plasma membranes, 50 oocytes were injected with 10 ng of cRNA per oocyte of rOct1-FLAG or rOct1(G478C)-FLAG and incubated for 2 days at 16 °C for expression. Plasma membranes of the oocytes were isolated by differential centrifugation according to Kamsteeg and Deen (27) as described earlier (28).

*SDS-PAGE and Western Blotting*—For SDS-PAGE, protein samples were treated for 30 min at 37 °C in 60 mM Tris-HCl, pH 6.8, 100 mM dithiothreitol, 2% (w/v) SDS, and 7% (v/v) glycerol. SDS-PAGE and staining with Coomassie Brilliant Blue were performed as described (29). Proteins from polyacrylamide gels were transferred to polyvinylidene difluoride membranes by electroblotting and immunostaining was performed as described (20). Anti-FLAG antibody (from Sigma), raised in mice, diluted 1:20,000 was used as primary antibody. Anti-mouse IgG coupled to HRP from Sigma (1:5,000) was used as secondary antibody. Binding of HRP-coupled antibodies was visualized using enhanced chemiluminescence (ECL system; Amersham Biosciences). For determination of apparent molecular masses, prestained molecular weight markers (BenchMark) from Invitrogen were employed. Staining of proteins in

Western blots was quantified by densitometry as described (30).

*Calculations and Statistics*—For measurements in oocytes, at least three different batches of oocytes were used. For uptake measurements with radioactive substrates, 8–10 oocytes were analyzed per experimental condition and oocyte batch. Uptake rates determined in HEK293 cells were performed in at least three different experiments in which four individual measurements were performed per experimental condition. The software package GraphPad Prism Version 4.1 (GraphPad Software, San Diego) was used to compute statistical parameters. Apparent $K_m$ values and concentrations for half-maximal activation of currents ($I_{0.5}$) were determined by fitting the Michaelis-Menten equation to the data. For inhibition of tracer cation uptake by nonlabeled cations $IC_{0.5}$ values were calculated by fitting the Hill equation to the data. Because the $MPP^+$ concentrations used for uptake measurements in inhibition studies were at least 10 times smaller compared with the $K_m$ value for $MPP^+$, the $IC_{50}$ values are basically identical to $K_i$ values. The time constants ($\tau$) of voltage-dependent fluorescence changes were determined as described by fitting a biexponential function to the data using IgorPro Version 6.0 (13). Mean values ± S.E. are indicated. Analysis of variance test with post hoc Tukey comparison was used to compare more than two different groups. Two-sided Student's *t* test was used to prove statistical significance of differences between two groups. $p$ values $< 0.05$ were considered as statistically significant. Fluorescence recordings were corrected for photo-bleaching and analyzed using IgorPro Version 6.0 (WaveMetrics Inc., Lake Oswego, OR).

## RESULTS

*Potential- and Cation-dependent Movements of Amino Acids in TMHs 5, 8, and 11 of rOct1*—Previously, we identified two amino acids (Phe-483 and Phe-486) in the 11th TMH, which moved in response to changes of the membrane potential and to interaction of organic cations with the transporter (13). The movements were detected by voltage clamp fluorometry on *X. laevis* oocytes expressing rOct1 mutants that were labeled with a fluorescent dye. In the mutants, 10 endogenous cysteine residues had been replaced (rOct1(10ΔC), Phe-483 or Phe-486 were then replaced by cysteine, and F483C or F486C were subsequently covalently labeled with tetramethylrhodamine maleimide (TMRM). Voltage-dependent and ligand-dependent fluorescence changes were observed for both labeled mutants. In this study, we could not distinguish whether the observed movements represented a selective movement of TMH 11 that contains two amino acids that bind $TEA^+$ (14, 15) or whether the observed movements are part of major conformational changes involving several TMHs. To answer this question, we individually replaced various amino acids of rOct1(10ΔC) in the outer parts of TMH 5 (Val-255, Tyr-257, Pro-260, Asp-261, Trp-262, and Arg-263) and TMH 8 (Tyr-377, Asp-379, Phe-380, Phe-381, and Tyr-382) by cysteine residues (supplemental Fig. 1), labeled the introduced cysteines with TMRM, and tested the labeled mutants for voltage-dependent fluorescence changes. All mutants could be functionally expressed in oocytes; however, mutants Y257C, W262C, P263C, and Y377C showed largely reduced transport activities compared with rOct1(10ΔC) (supplemental Fig. 2). Voltage-dependent fluorescence changes were only observed after TMRM labeling of rOct1(10ΔC,C260) and rOct1(10ΔC,C380) (Fig. 1, *B* and *C*, and supplemental Fig. 3). The fluorescence of both mutants decreased with increasing membrane potential. At variance, fluorescence increased with increasing membrane potential after TMRM labeling of rOct1(10ΔC,C483)[3] (Fig. 1*D*). The data indicate bulk conformational changes in response to the changes in membrane potential.

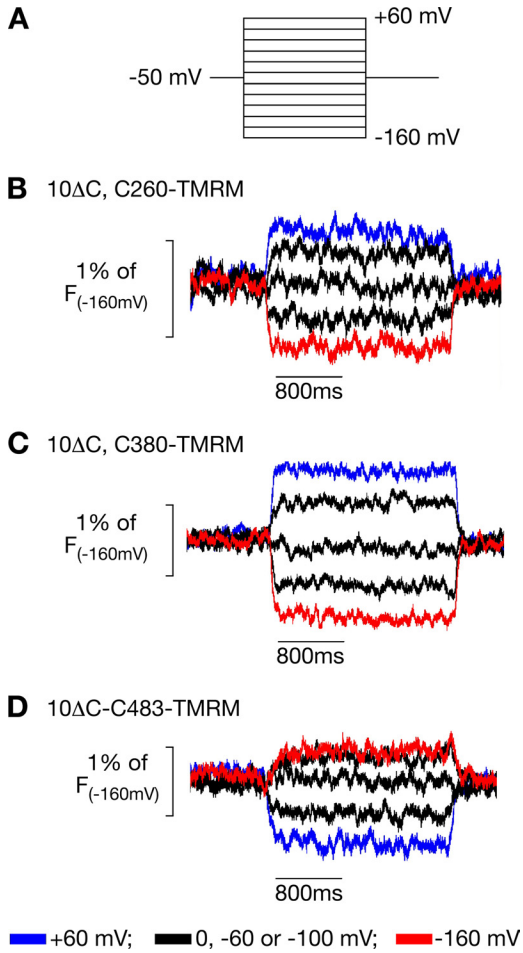


FIGURE 1. **Voltage-dependent fluorescence changes of TMRM-labeled amino acids in three TMHs.** Mutants rOct1(10ΔC,P260C), rOct1(10ΔC,F380C), and rOct1(10ΔC,F483C) were expressed in *X. laevis* oocytes and labeled with TMRM. Starting from −50 mV, the oocytes were clamped to 12 different potentials as indicated in *A*, and the fluorescence was recorded. *B–D*, five representative original fluorescence recordings of each of the three mutants are shown.

Testing whether the observed conformational changes may be relevant for translocation, we investigated whether the voltage-dependent fluorescence changes observed with TMRM-labeled rOct1(10ΔC,C260) and rOct1(10ΔC,C380) were affected by the presence of saturating concentrations of the substrates $choline^+$ and $MPP^+$ and the nontransported inhibitor $TBuA^+$ as observed for rOct1(10ΔC,C483-TMRM) (13). Also in these variants, the voltage-dependent fluorescence

[3] In our previous experiments showing that the fluorescence of TMRM-labeled rOct1(10ΔC-F483C) decreased with increasing membrane potential (13), the polarity was interchanged.

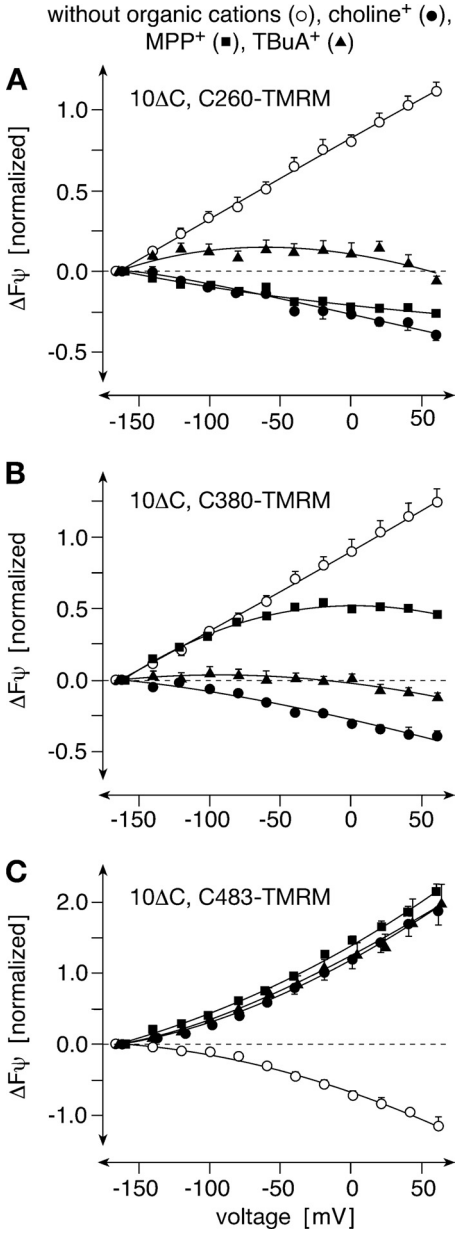


FIGURE 2. **Effects of organic cations on voltage-dependent fluorescence changes of rOct1(10ΔC,C260-TMRM), rOct1(10ΔC,C380-TMRM), and rOct1(10ΔC,F483-TMRM).** The rOct1 mutants were expressed in oocytes and superfused with Ori buffer (without organic cations), Ori buffer containing 10 mM choline (*choline*$^+$), 100 $\mu$M MPP$^+$ (*MPP*$^+$), or 100 $\mu$M TBuA$^+$ (*TBuA*$^+$). Means ± S.E. of 5–8 oocytes from three different oocyte batches are indicated.

changes were influenced by organic cations (Fig. 2). In contrast to rOct1(10ΔC,C483-TMRM) where all three organic cations reversed decrease of the voltage-dependent fluorescence in the same way (Fig. 2*C*), choline$^+$, MPP$^+$, and TBuA$^+$ exhibited different effects in rOct1(10ΔC,C260-TMRM) (Fig. 2*A*) and rOct1(10ΔC,C380-TMRM) (Fig. 2*B*). Whereas choline$^+$ reversed the voltage-dependent fluorescence changes in rOct1(10ΔC,C260-TMRM) and rOct1(10ΔC,C380-TMRM), MPP$^+$ reversed the voltage-dependent fluorescence of rOct1(10ΔC,C260-TMRM) but only reduced the potential-dependent fluorescence change of rOct1(10ΔC,C380-TMRM) between −50 mV and +50 mV. TBuA$^+$ abolished the voltage-dependent fluorescence changes in rOct1(10ΔC,C260-TMRM) and rOct1(10ΔC,C380-TMRM) in a similar way. The data suggest that the described conformational changes occur during binding and/or translocation of organic cations. They are consistent with the alternating access transport model that predicts that membrane potential and ligand binding influence the equilibrium between outward-open and inward-open transporter conformations. The differential effects obtained with two different substrates and the effects of the nontransported inhibitor TBuA$^+$ on bulk movements suggest a high complexity of structural transitions during binding and translocation.

*Functional Characterization of the rOct1(10ΔC) Mutants and Their Modification with TMRM*—For interpretation of the observed fluorescence changes, various controls were required. Although Pro-260, Phe-380 and Phe-483 are located in the outer part of the large binding cleft of rOct1 (4), replacement of these amino acids by cysteine residues and/or their modification by TMRM may change functional properties of the transporter. To characterize functions of the employed variants, we compared the concentration dependences of choline$^+$-induced currents ($I_{0.5}$), of [$^3$H]MPP$^+$ uptake ($K_m$) and of inhibition of [$^3$H]MPP$^+$ uptake by TBuA$^+$ ($IC_{50}$) between rOct1(10ΔC,P260C), rOct1(10ΔC,F380C), rOct1(10ΔC,F483C), and rOct1(10ΔC) (Table 1 and supplemental Fig. 4). All four mutants exhibited similar $I_{0.5}$ values of choline$^+$-induced currents at −50 mV. Similar $K_m$ values of MPP$^+$ uptake were obtained for rOct1(10ΔC), rOct1(10ΔC,P260C), and rOct1(10ΔC,F380C); however, the $K_m$ value for rOct1(10ΔC,F483C) was 2-fold smaller. The $IC_{50}$ values for inhibition of MPP$^+$ uptake by TBuA$^+$ were comparable between rOct1(10ΔC) and rOct1(10ΔC,P260C), 2-fold smaller in rOct1(10ΔC,F380C) in comparison with rOct1(10ΔC), and 10-fold smaller in rOct1(10ΔC,F483C). The data suggest that the observed MPP$^+$-induced fluorescence changes in position 483 and the TBuA$^+$-induced fluorescence changes in positions 380 and 483 are influenced by the mutations in these positions.

To determine whether the TMRM modifications of the introduced cysteines influence functional properties, we incubated the mutants for 5 min with 250 $\mu$M TMRM, washed the oocytes, and measured MPP$^+$ uptake and inhibition of MPP$^+$ uptake by TBuA$^+$. To ensure complete modification of the cysteines, we used a 7.5-fold longer incubation time as has been used for voltage clamp fluorometry and a 25-fold higher concentration of TMRM. After TMRM modification, uptake rates of 2.5 nM [$^3$H]MPP$^+$, $K_m$ values of MPP$^+$ uptake, and $IC_{50}$ values for inhibition of MPP$^+$ uptake by TBuA$^+$ were not changed significantly (supplemental Fig. 5*A* and Table 1). The data indicate that the attached fluorescent dye did not alter transporter function and suggest that the observed fluorescence changes represent movements of the unmodified transporter.

*Exchange of Glycine 478 by Cysteine Renders rOCT1(10ΔC) Susceptible to Irreversible Inhibition by a Transported Sulfhydryl Reagent*—To identify transport related conformational changes, we generated a mutant with a cysteine residue in the transport path that can be modified by the transported sulfhydryl reagent MTSET$^+$ to block transport activity during voltage clamp fluorescence experiments. Transport of MTSET$^+$ by

**TABLE 1**

**Functional characteristics of rOct1(10ΔC) after replacements of Gly-478 in the transport path and/or of Pro-260, Phe-380, and Phe-483 in peripheral positions by cysteine residues and after TMRM modification of the peripheral cysteines**

The indicated mutants were expressed in oocytes, and part of them were incubated for 5 min with 250 $\mu$M TMRM. In oocytes clamped to −50 mV, currents were measured that were induced by various concentrations of choline. The concentrations required for half-maximal activations ($I_{0.5}$) were calculated by fitting the Michaelis equation to the data. The number of analyzed oocytes are indicated in parentheses. For $K_m$ determinations, uptake of 10 nM [$^3$H]MPP$^+$ was measured in the presence of different concentrations of nonradioactive MPP$^+$ and corrected for uptake in oocytes in which no transporter was expressed. $K_m$ values were calculated by fitting the Michaelis-Menten equation to the data. The number of independent experiments in which 8–10 oocytes were measured per MPP$^+$ concentration are indicated in parentheses. For determinations of half-maximal concentrations ($IC_{50}$) for inhibition of MPP$^+$ uptake by TBuA$^+$, uptake of 2.5 nM [$^3$H]MPP$^+$ was measured in the presence of different concentrations of TBuA$^+$. The $IC_{50}$ values of individual experiments in which 8–10 oocytes were analyzed per TBuA$^+$ concentration were calculated by fitting the Hill equation to the data. The numbers of independent experiments are indicated in parentheses. Mean values ± S.E. are indicated. *, $p < 0.05$; **, $p < 0.01$; ***, $p < 0.001$ difference to rOct1(10ΔC) calculated by analysis of variance with post hoc Tukey comparison.

| Variant | $I_{0.5}$ of choline$^+$-induced current | $K_m$ of MPP$^+$ uptake | $IC_{50}$ for inhibition of MPP$^+$ uptake by TBuA$^+$ |
|---|---|---|---|
| | mM | μM | μM |
| rOct1(10ΔC) | 1.28 ± 0.10 (6) | 8.64 ± 1.05 (5) | 22.94 ± 0.86 (5) |
| rOct1(10ΔC,G478C) | 0.92 ± 0.05 (5) | 7.48 ± 0.84 (3) | 8.71 ± 1.86 (3)*** |
| rOct1(10ΔC,P260C) | 1.52 ± 0.35 (5) | 9.53 ± 1.62 (3) | 20.94 ± 3.28 (3) |
| rOct1(10ΔC,P260C) TMRM | | 9.19 ± 1.39 (3) | 22.90 ± 4.35 (3) |
| rOct1(10ΔC,P260C,G478C) | 1.42 ± 0.29 (5) | 10.48 ± 0.65 (3) NS[a] | 10.39 ± 0.35 (3)*** S[b] |
| rOct1(10ΔC,F380C) | 1.54 ± 0.04 (5) | 8.10 ± 1.15 (3) | 12.07 ± 0.68 (3)** |
| rOct1(10ΔC,F380C) TMRM | | 8.82 ± 1.29 (3) | 11.54 ± 1.01 (3)** |
| rOct1(10ΔC,F380C,G478C) | 1.54 ± 0.13 (5) | 6.70 ± 0.37 (3) NS[a] | 8.72 ± 1.35 (3)*** NS[a] |
| rOct1(10ΔC,F483C) | 1.30 ± 0.16 (10)[c] | 4.07 ± 0.80 (3)* | 2.09 ± 0.74 (3)*** |
| rOct1(10ΔC,F483C)TMRM | | 4.33 ± 0.61 (3)* | 4.24 ± 1.12 (3)*** |
| rOct1(10ΔC,F483C,G478C) | 1.45 ± 0.16 (4) | 4.17 ± 0.67 (3)* NS[a] | 2.82 ± 1.00 (3)*** NS[a] |

[a] NS means not significant as determined by Student's *t* test compared to the respective nonlabeled variant without G478C mutation.
[b] S means $p < 0.01$ compared to rOct1(10ΔC, P260C) determined by Student's *t* test.
[c] These data have been previously reported (13).

rOct1 wild type and rOct1(10ΔC) could be demonstrated (Fig. 3*A*). For MTSET$^+$ uptake by rOct1(10ΔC), a $K_m$ value of 0.53 ± 0.05 mM ($n = 3$) was determined (Fig. 3*B*). We replaced the amino acids Gly-478, Thr-481, Val-485, Phe-486, Arg-487, Leu-488, Met-489, and Glu-490 in rOct1(10ΔC) by cysteine residues and measured the irreversible inhibition of [$^{14}$C]TEA transport by MTSET$^+$ (supplemental Fig. 6). Significant inhibition was observed with rOct1(10ΔC,G478C) and rOct1(10ΔC,T481C). The data suggest that these cysteine residues are located in the transport path and that their modification inhibits or blocks transport.

*Exchange of Glycine 478 by Cysteine Changed Turnover for MPP$^+$ and Affinity for TBuA$^+$*—Because Gly-478 is located one α-helix turn above Cys-474 and Asp-475, which are supposed to be directly involved in substrate binding (15, 16) and may allow bending of TMH11, we wondered whether Gly-478 is directly involved in the transport mechanism. We investigated whether the G478C mutation altered the functional properties of the transporter. After replacements of glycine 478 by cysteine in rOct1(10ΔC) and rOct1(10ΔC,P260C), the concentrations for half-maximal inhibition ($IC_{50}$) of the [$^3$H]MPP$^+$ (2.5 nM) uptake by TBuA$^+$ were decreased by 62 and 50%, respectively (Table 1 and supplemental Fig. 7*B*). In the mutants rOct1(10ΔC,F380C) and rOct1(10ΔC,F483C), which exhibited a decreased $IC_{50}$ for inhibition of [$^3$H]MPP$^+$ uptake by TBuA$^+$ compared with rOct1(10ΔC), the replacement of glycine 478 by cysteine did not lead to a further increase of the respective $IC_{50}$ values for TBuA$^+$ (Table 1). We also compared $K_m$ values for MPP$^+$ uptake and inhibition of MPP$^+$ (0.1 μM) uptake by TBuA$^+$ in HEK293 cells that were stably transfected with rOct1(10ΔC) or rOct1(10ΔC,G478C) (supplemental Figs. 7*C* and 8*A*). Notably, after expression of rOct1 or rOct1 mutants in oocytes or HEK293 cells, similar $K_m$ values were obtained for MPP$^+$ uptake, whereas the $IC_{50}$ values of inhibition of MPP$^+$

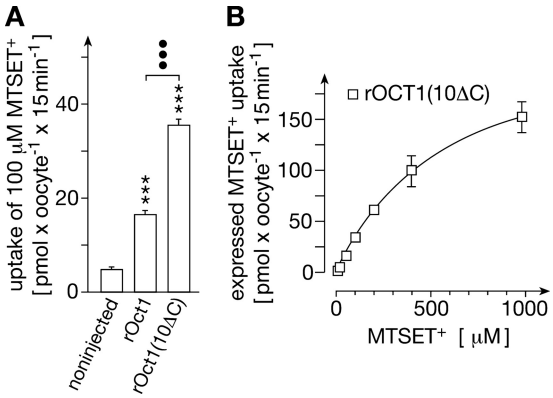


FIGURE 3. **Sulfhydryl reagent MTSET$^+$ is transported by rOct1 and rOct1(10ΔC).** Noninjected oocytes, oocytes injected with rOct1 cRNA, or oocytes injected with rOct1(10ΔC) cRNA were incubated for 3 days. For transport measurements, the oocytes were incubated 15 min with [$^{14}$C]MTSET$^+$ plus different concentrations of nonradioactive MTSET$^+$ and washed, and the MTSET$^+$ concentrations in the oocytes were measured. *A,* comparison of MTSET$^+$ uptake in noninjected oocytes, oocytes expressing rOct1, and oocytes expressing rOct1(10ΔC). *B,* substrate dependence of rOct1(10ΔC)-mediated MTSET$^+$ uptake. MTSET$^+$ uptake into rOct1(10ΔC) expressing oocytes was measured at different MTSET$^+$ concentrations and corrected for uptake in noninjected oocytes. Mean values ± S.E. of 24–27 oocytes from three independent experiments are indicated. ***, $p < 0.001$ for difference to noninjected oocytes. ●●●, $p < 0.001$ for difference between the indicated groups. The curve in *B* was obtained by fitting the Michaelis-Menten equation to the data.

uptake by TBuA$^+$ were lower after expression in HEK293 cells compared with oocytes (supplemental Fig. 8*B*). For example, the $IC_{50}$ value of inhibition of MPP$^+$ uptake by TBuA$^+$ expressed by rOct1(10ΔC) was 15-fold lower in HEK293 cells (0.44 ± 0.06 μM, $n = 3$) compared with oocytes (22.9 ± 0.9 μM, $n = 5$, $p < 0.001$ for difference). The differences in affinity for TBuA$^+$ observed in the different expression systems are probably due to different regulatory states of the transporter (31). As observed in oocytes also in HEK293 cells, the $K_m$ value for MPP$^+$ uptake expressed by rOct1(10ΔC) was not altered by the G478C exchange (rOct1(10ΔC), 5.4 ± 0.7 μM, $n = 3$;

rOct1(10ΔC,G478C), 3.8 ± 1.1 μM, $n = 3$, differences not significant), whereas the $IC_{50}$ value for inhibition of $MPP^+$ uptake by $TBuA^+$ was decreased by a similar degree as in oocytes (rOct1(10ΔC), 1.5 ± 0.3 μM, $n = 3$; rOct1(10ΔC,G478C), 0.44 ± 0.06 μM, $n = 3$, $p < 0.01$) (supplemental Fig. 8*B*). The data suggest that the G478C exchange does not alter the mechanism of $MPP^+$ transport but increases the affinity for binding of $TBuA^+$.

Targeted modifications of cysteines with TMRM and $MTSET^+$ had to be performed on the basis of rOct1(10ΔC) to avoid nonselective modifications. Because rOct1-(10ΔC) shows increased choline-induced currents and decreased affinity for $choline^+$ (18) and $TBuA^+$ (supplemental Fig. 8*B*), we investigated whether the effect of the mutation G478C in rOct1(10ΔC) on $TBuA^+$ affinity was also observed in the rOct1 wild type background. Because we additionally wanted to determine the effects of the G478C mutation on membrane expression, we used rOct1 wild type containing a FLAG tag at the C terminus for these experiments. We had verified that the FLAG tag had no effect on the affinities of this variant to $MPP^+$ or $TBuA^+$ (supplemental Fig. 8*A*). After exchanging glycine 478 with cysteine in rOct1-FLAG and expressing the variants in oocytes, the same effects were observed as for rOct1(10ΔC). Whereas the $K_m$ values for $MPP^+$ uptake were unaltered by the G478C mutation, the $IC_{50}$ value of inhibition of $MPP^+$ uptake by $TBuA^+$ was decreased (rOct1-FLAG, 6.78 ± 1.12 μM ($n = 4$); rOct1(G478C)-FLAG 0.43 ± 0.06 μM, $n = 4$ both, $p < 0.001$).

To determine whether the maximal rate of $MPP^+$ uptake was changed by the G478C mutation, we expressed FLAG-tagged rOct1 wild type and FLAG-tagged rOct1(G478C) in identical batches of oocytes and measured the $V_{max}$ values for $MPP^+$ uptake. In parallel, we purified plasma membranes by adsorption to colloidal silica (27), separated the plasma membrane proteins by SDS-PAGE, and identified the transporter proteins by Western blotting using an anti-FLAG antibody. Quantification of antibody staining revealed that the expression was unaltered by the G478C mutation (Fig. 4*A*). Because the $V_{max}$ value of $MPP^+$ uptake was reduced by 37% (Fig. 4*B*), the G478C exchange reduces the turnover of rOct1 for $MPP^+$ transport.

The data suggest that glycine 478 is part of the $TBuA^+$ binding domain within the outward-open cleft, and it is critical for velocity of transport.

*Mutation of Glycine 478 Alters Membrane Potential- and/or Cation-dependent Movements of Amino Acids in TMHs 5, 8, and 11*—Next, we determined whether the G478C exchange causes changes in membrane potential- and cation-induced structural changes of rOct1. Fig. 5 shows that the voltage-dependent movements in positions 260 (TMH 5) and 483 (TMH 11) were largely reduced by the G478C mutation, whereas the movement in position 380 was unchanged. G478C replacement changed cation effects in positions 260, 380, and 483 differently. After G478C exchange in rOct1(10ΔC,P260C), the effects of $choline^+$ and $MPP^+$ on the membrane potential-dependent fluorescence changes observed in rOct1(10ΔC,P260C) were abolished (compare Fig. 6*A* with Fig. 2*A*). The effect of $TBuA^+$ could not be determined because binding of $TBuA^+$ to TMRM-labeled rOct1(10ΔC,P260C,G478C) was not completely reversible. In rOct1(10ΔC,F380C,G478C), the $choline^+$-induced reduction of the voltage-dependent fluorescence increase was much smaller compared with rOct1(10ΔC,P380C) (compare Fig. 6*B* with Fig. 2*B*). The effects of $MPP^+$ and $TBuA^+$, however, were similar. In rOct1(10ΔC,F483C,G478C), which exhibited a much smaller voltage-dependent fluorescence change in the absence of organic cations, $TBuA^+$ did not alter the voltage-dependent fluorescence change in contrast to rOct1(10ΔC,F483C) (compare Fig. 6*C* with Fig. 2*C*).

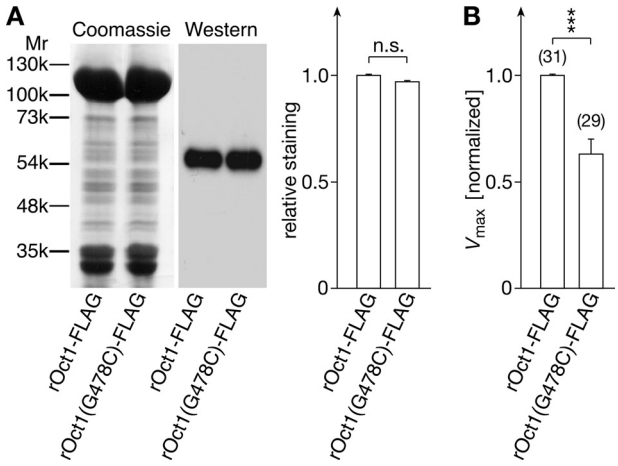


FIGURE 4. **Exchange of glycine 478 by cysteine in rOct1 decreases the turnover for $MPP^+$.** FLAG-tagged rOct1 wild type (*rOct1-FLAG*) or mutant (*rOct1*(*G478C*)-*FLAG*) were expressed in oocytes. *A,* plasma membranes of the oocytes were isolated, and the proteins were separated by SDS-PAGE. The gels were stained with Coomassie Brilliant Blue or analyzed in a Western blot using an anti-FLAG antibody. The densities of the antibody-stained bands were quantified by densitometry. Mean values ± S.E. of three experiments are indicated. *B,* comparison of $V_{max}$ values of $MPP^+$ uptake mediated by rOct1-FLAG and rOct1(G478C)-FLAG. Uptake of 0.1 μM [$^3$H]$MPP^+$ in oocytes expressing rOct1-FLAG or rOct1(G478C)-FLAG or in noninjected oocytes were measured, and the transporter expressed uptake rates were calculated. The $V_{max}$ values were calculated according to the Michaelis-Menten equation using the $K_m$ values that were determined in separate experiments (rOct1-FLAG 7.75 ± 1.17 μM and rOct1(G478C)-FLAG 5.23 ± 0.61 μM ($n = 3$ each)). Mean values ± S.E. are indicated. The number of analyzed oocytes is indicated in *parentheses*. Three independent experiments using different oocytes batches were performed. The uptake rates were normalized to the mean values of $MPP^+$ uptake in rOct1-FLAG-expressing oocytes of the respective experiment. ***, $p < 0.001$. *n.s.,* not significant.

Because a low concentration of the fluorescent sulfhydryl reagent TMRM was employed for modification, which should only modify a small fraction of the transporter molecules and as cysteine 478 is located relatively deep within the outside open transport cleft, it seemed unlikely that cysteine 478 would be modified in addition to cysteines 260, 380, or 483 in rOct1(10ΔC,P260C,G478C), rOct1(10ΔC,F380C,G478C), or rOct1(10ΔC,F483C,G478C). However, we also wondered why the replacement of glycine 478 by cysteine altered the voltage-dependent fluorescence in rOct1(10ΔC,P260C,G478C) and rOct1(10ΔC,F483C,G478C) to such a dramatic extent (Fig. 5, *A* and *C*); nevertheless, the theoretical possibility of TMRM modification of cysteine 478 had to be excluded. Therefore, we generated the mutant rOct1(10ΔC,F483C,G478S), expressed it in oocytes, labeled it with TMRM, and measured voltage-dependent fluorescence changes (Fig. 7*A*). The data were very similar to those obtained with rOct1(10ΔC,F483C,G478C). The voltage-dependent decrease of fluorescence observed

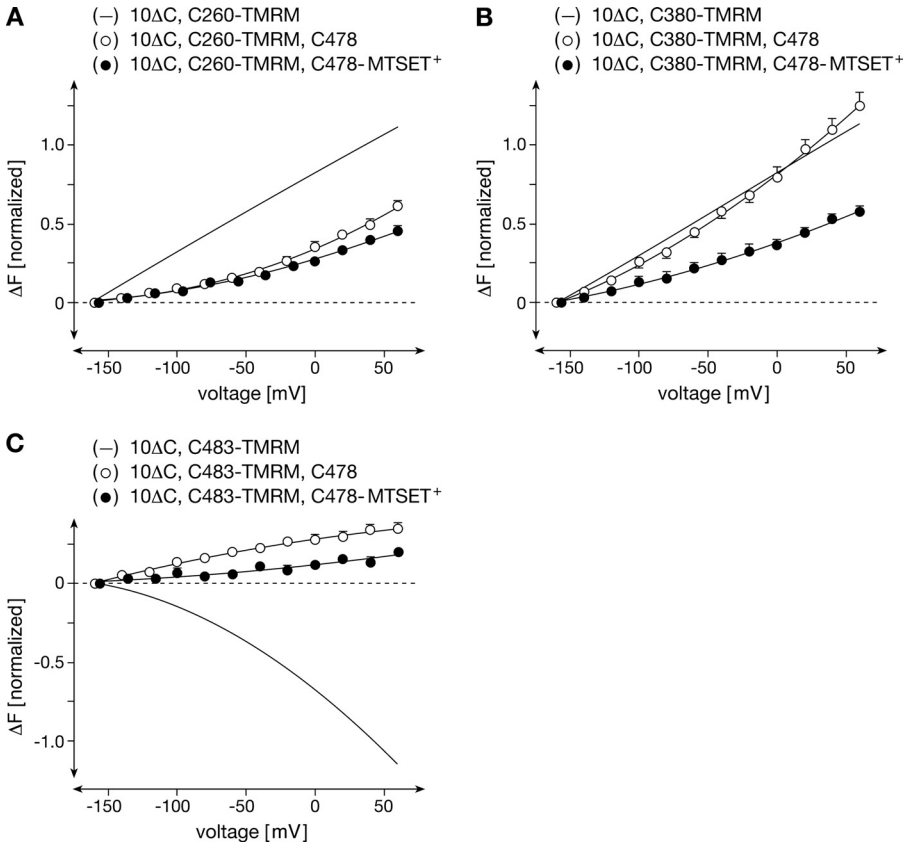


FIGURE 5. **G478C mutation alters voltage-dependent movements of C260-TMRM and C483-TMRM in absence of organic cations, whereas MTSET$^+$ modification of Cys-478 alters voltage-dependent movement of C380-TMRM.** rOct1(10ΔC, P260C), rOct1(10ΔC, P260C,G478C), rOct1(10ΔC,F380C), rOct1(10ΔC,F380C,G478C), rOct1(10ΔC,F483C), and rOct1(10ΔC,F483C,G478C) were expressed in oocytes. All oocytes were labeled with TMRM. In part of the oocytes, voltage-dependent fluorescence changes were measured after TMRM labeling. The fluorescence measurements with rOct1(10ΔC,C260-TMRM), rOct1(10ΔC,C380-TMRM), and rOct1(10ΔC,C483-TMRM) are indicated as *lines* (for individual measurements see Fig. 2). Part of the oocytes expressing rOct1(10ΔC,P260C,G478C), rOct1(10ΔC,F380C,G478C), and rOct1(10ΔC,F483C,G478C) was additionally modified with MTSET$^+$, and voltage-dependent fluorescence changes were analyzed. Mean values ± S.E. of 4–6 oocytes from three different oocyte batches are indicated.

with rOct1(10ΔC,F483C) was reversed to an increase of fluorescence.

To determine whether the rate of the voltage-dependent fluorescence changes of TMRM-labeled cysteine 483 is altered by the mutations at position 478, we measured the half-times of voltage-dependent fluorescence changes ($\tau$) in rOct1(10ΔC, F483C), rOct1(10ΔC,F483C,G478C), and rOct1(10ΔC,F483C, G478S), as described previously (13). Similar time constants were obtained for "on" and "off" rates. Fitting of the time courses to biexponential curves provided distinguishable $\tau$ values for relatively fast changes (~50 ms) and for more slow changes (~120 ms) only for rOct1(10ΔC,F483C). For rOct1(10ΔC,F483C,G478C) and rOct1(10ΔC,F483C, G478S), only one constant for a fast voltage-dependent change of fluorescence ($\tau$ ~25 ms) was determined. In Fig. 7*B*, the $\tau$ values for the relatively fast fluorescence changes observed for the three mutants are compared. Significantly smaller $\tau$ values were obtained for rOct1(10ΔC,F483C,G478C) and rOct1(10ΔC, F483C,G478S) compared with rOct1(10ΔC, F483C), indicating that the voltage-dependent movement of the amino acid in position 483 is more rapid if Gly-478 is exchanged by cysteine or serine. The data indicate that glycine 478 is located at a position that is critical for membrane potential-dependent and cation-dependent conformational changes, which are supposed to occur during transport.

*Irreversible Blockage of Organic Cation Transport by rOct1 after Covalent Modification of rOct1(10ΔC,G478C) by the Transported Sulfhydryl Reagent MTSET$^+$*—When oocytes expressing rOct1(10ΔC,G478C) were incubated for 10 min at room temperature with Ori buffer containing 100 $\mu$M MTSET$^+$ and washed extensively, organic cation transport uptake was reduced by about 70%, whereas it was unaltered when rOct1(10ΔC) was treated with MTSET$^+$ (Fig. 8, *A*, *B*, and *D*). Cation transport expressed by rOct1 mutants was determined by measuring uptake of 9 $\mu$M [$^{14}$C]TEA$^+$ (Fig. 8*A*) and currents that were induced by superfusion of the oocytes with 1 mM TEA$^+$ (Fig. 8*B*) or 10 mM choline$^+$ (Fig. 8*D*). Because we could not achieve 100% inhibition of transport after 10 min of incubation with MTSET$^+$, we wondered whether the remaining activity is due to residual transport activity of MTSET$^+$-labeled transporters or represents activity of nonlabeled transporter molecules. Reasoning that residual activity of the MTSET$^+$-labeled transporter may exhibit altered affinities for substrates and/or inhibitors in addition to reduced turnover, we measured the effects of covalent MTSET$^+$ labeling of rOct1(10ΔC) or rOct1(10ΔC,G478C) onto the $K_m$ values for MPP$^+$ uptake and onto the $IC_{50}$ values for inhibition of MPP$^+$ uptake by TBuA$^+$. Because these measurements could not be determined with sufficient accuracy in oocytes, they were performed in HEK293 cells that were stably transfected with rOct1(10ΔC) or

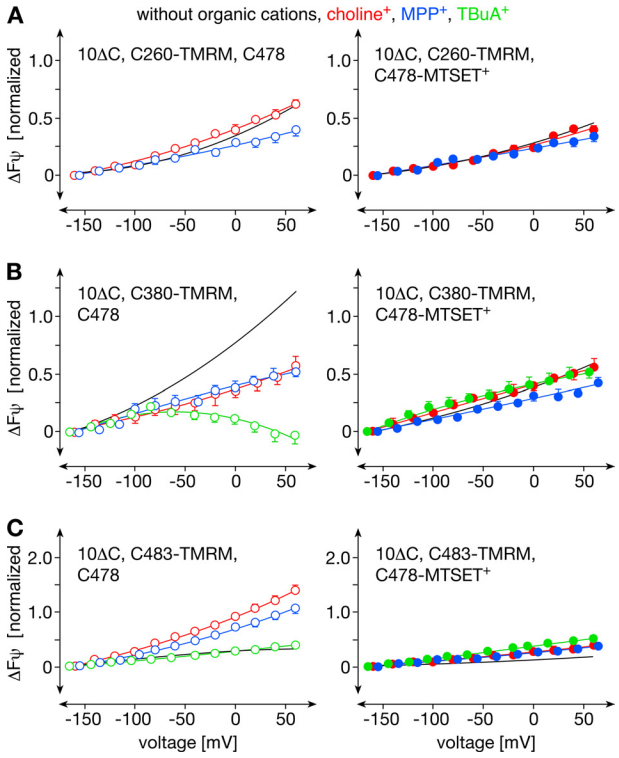


FIGURE 6. **Effects of organic cations on voltage-dependent movements of TMRM-labeled C260-TMRM, C380-TMRM, and C483-TMRM in the rOct1(10ΔC,G478C) mutant without and with modification of Cys-478 with MTSET$^+$.** rOct1(10ΔC,P260C,G478C), rOct1(10ΔC,F380C,G478C), and rOct1(10ΔC,F483C,G478C) were expressed in oocytes, and Cys-260, Cys-380, and Cys-483 were modified with TMRM. In part of the oocytes, additional modification of Cys-478 with MTSET$^+$ was performed. The oocytes were superfused with Ori buffer (without organic cations) or Ori buffer containing 10 mM choline (*choline*$^+$), 100 $\mu$M MPP$^+$ (*MPP*$^+$), or 100 $\mu$M TBuA$^+$ (*TBuA*$^+$). Measurements performed without organic cations are indicated by *lines* (for individual values see Fig. 5). Means ± S.E. of 4–6 oocytes from three different oocyte batches are indicated. The data show that the effects of organic cations were reduced and partially abolished by the G478C mutation and totally abolished after MTSET$^+$ labeling of Cys-478.

rOct1(10ΔC,G478C). For covalent modification, the cells were incubated with 1 mM MTSET$^+$ for 1 min at room temperature and subsequently washed. After this treatment, the $V_{max}$ of MPP$^+$ uptake into HEK293 cells expressing rOct1(10ΔC) was unaltered, although it was decreased by about 90% in HEK293 cells expressing rOct1(10ΔC,G478C) (supplemental Fig. 9*A*). After MTSET$^+$ treatment, neither the $K_m$ values for MPP$^+$ uptake nor the $IC_{50}$ values for inhibition of MPP$^+$ uptake by TBuA$^+$ were changed in both cell lines (supplemental Fig. 9, *B* and *C*). The data suggest that the residual activity after MTSET$^+$ labeling of cells expressing rOct1(10ΔC,G478C) was due to unlabeled transporter molecules.

*Covalent Modification of rOct1(10ΔC,G478C) with MTSET$^+$ Blocks MPP$^+$ Binding*—To differentiate whether the covalent modification of cysteine 478 by MTSET$^+$ prevents substrate binding or blocks transport-related conformational changes, we investigated whether the binding of MPP$^+$ to the outward-open conformation was changed after MTSET$^+$ labeling of rOct1(10ΔC,G478C). The measurements were performed at 0 °C with HEK293 cells that were stably transfected with rOct1(10ΔC) or rOct1(10ΔC,G478C). Nonsaturable binding of [$^3$H]MPP$^+$ in the presence of 5 mM nonradioactive MPP$^+$ was subtracted.[4] Binding of [$^3$H]MPP$^+$ to rOct1(10ΔC) without and with MTSET$^+$ treatment was similar to rOct1(10ΔC,G478C) without MTSET$^+$ treatment; however, no binding of [$^3$H]MPP$^+$ could be detected in HEK293 cells expressing rOct1(10ΔC,G478C) that had been treated with MTSET$^+$ (Fig. 9*A*). The data indicate that the modification of Cys-478 by MTSET$^+$ blocks transport by preventing MPP$^+$ binding to the outward-open conformation. For MPP$^+$ binding to rOct1(10ΔC) and rOct1(10ΔC,G478C), $K_D$ values of 3.52 ± 0.33 ($n$ = 4) and 2.93 ± 0.27 ($n$ = 4) $\mu$M were determined (Fig. 9*B*). Because the $K_D$ values do not differ significantly from the respective Michaelis-Menten constant ($K_m$) values for MPP$^+$ uptake, the $K_m$ values are mainly determined by the binding affinity of MPP$^+$.

*Covalent Modification of rOct1(10ΔC,G478C) with MTSET$^+$ Alters Voltage-dependent Structural Changes and Blocks Cation-induced Structural Changes*—Voltage clamp fluorometry showed that MTSET$^+$ modification of Cys-478 did not alter voltage-dependent fluorescence changes in positions 260 (TMH 5) and 483 (TMH 11) significantly (Fig. 6, *A* and *C*). In contrast, MTSET$^+$ labeling of Cys-478 blunted the voltage-dependent fluorescence increase of TMRM-labeled Cys-380 (TMH 8) (Fig. 6*B*). Consistent with the observation that MTSET$^+$ modification of Cys-478 prevents MPP$^+$ binding, no effects of MPP$^+$ on voltage-dependent fluorescence changes in positions 260, 380, and 483 were observed when Cys-478 was modified with MTSET$^+$ (Fig. 6). Similarly, no fluorescence changes in the three positions could be induced by choline$^+$ or TBuA$^+$. Substrate effects on voltage-dependent conformational changes in organic cation transporters can also be registered by capacitance measurements (26). After modification of Cys-478 with MTSET$^+$, the capacitance changes also induced by TEA$^+$ or choline$^+$ were abolished (Fig. 8, *C* and *E*).

*Membrane Potential- and Substrate-dependent Accessibility of Cysteine 478*—The above described data indicate that Gly-478 is critically involved in membrane potential-dependent structural changes of rOct1. These structural changes probably occur during transport because they are modified or blunted in the presence of substrates. The critical role of Gly-478 during the structural changes implies that the position of Gly-478 changes during the transport cycle. We thus tested whether the accessibility of Cys-478 for modification with MTSET$^+$ is dependent on the membrane potential and influenced by transported substrates that change the equilibrium of conformational states at a given membrane potential. We confirmed that Gly-478 is accessible from the extracellular side as predicted by the outward-open structural model of rOct1 (12, 18) by demonstrating that modification of Cys-478 by MTSET$^+$ was possible at 0 °C at which major structural changes can be precluded (see supplemental Fig. 10). To determine the accessibility of cysteine 478 at different membrane potentials, oocytes expressing rOct1(10ΔC,G478C) were clamped to −50 mV, and cur-

[4] The validity of this method to measure MPP$^+$ binding rather than slow uptake was demonstrated by showing that, in contrast to MPP$^+$ binding at 0 °C, MPP$^+$ uptake measured within 1 s at 37 °C could not be removed when the cells were cooled down to 0 °C and incubated for 5 min with 5 mM nonradioactive MPP$^+$ (S. Rehman, N. Gottlieb, V. Gorboulev, and H. Koepsell, unpublished data).

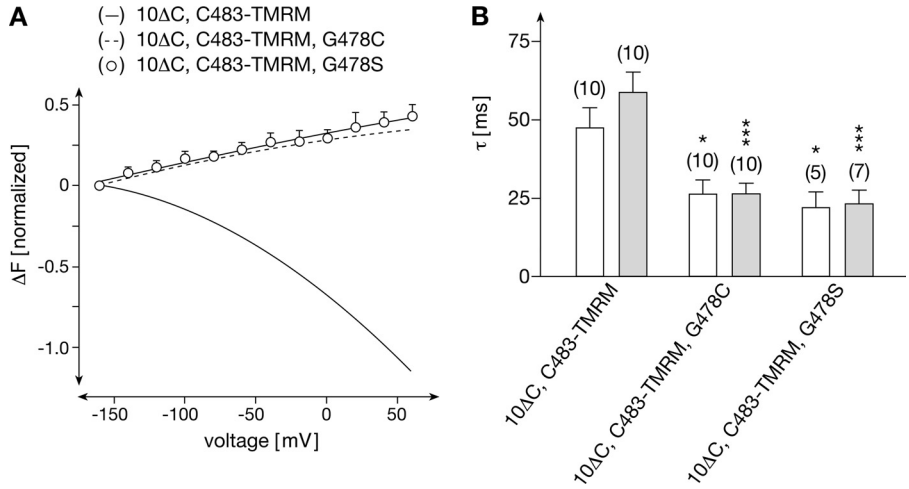


FIGURE 7. **Exchange of glycine 478 by cysteine or serine reverses voltage-dependent fluorescence changes of C478-TMRM but also alters the velocity of the voltage-dependent fluorescence changes.** rOct1(10ΔC,F483C), rOct1(10ΔC,F483C,G478C), and rOct1(10ΔC,F483C,G478S) were expressed in oocytes and modified by TMRM. *A,* comparison of voltage-dependent fluorescence changes. Measurements with rOct1(10ΔC,C483-TMRM) and rOct1(10ΔC,C483-TMRM,G478C) are indicated by *lines* (for individual measurements see Figs. 2*C* and 5*C*, respectively). The measurements were performed and are presented as in Fig. 2. *B,* onset of voltage-dependent fluorescence changes after switching the membrane potential from −50 to +60 mV (*open columns*) or from −50 to −160 mV (*closed columns*). The half-times for the fluorescence changes ($\tau$) are indicated. Means ± S.E. are shown. The numbers of measured oocytes are indicated in *parentheses*. *, $p < 0.05$; ***, $p < 0.001$ difference to rOct1(10ΔC,C483-TMRM) measured under the respective conditions. With rOct1(10ΔC,C483-TMRM), a slow phase of the potential-induced fluorescence changes $\tau$ values of 135 ± 10 ms (from −50 mV to +60 mV) and 118 ± 13 ms (from −60 mV to −160 mV) ($n = 10$, each) could be distinguished.

rents induced by superfusion with 10 mM choline were measured. The oocytes were washed with Ori buffer, clamped to different membrane potentials (0, −50, and −100 mV), and incubated for 45 s with Ori buffer containing 50 $\mu$M $MTSET^+$. After washing, the oocytes were clamped again to −50 mV, and the inward currents induced by 10 mM choline were measured (Fig. 10*A*). The irreversible inhibition of $choline^+$-induced currents by $MTSET^+$ was significantly lower at 0 mV compared with −50 or −100 mV indicating membrane potential-dependent changes of Cys-478 accessibility. To determine whether substrates change the accessibility of Cys-478, we clamped oocytes expressing rOct1(10ΔC,G478C) to −50 mV and measured the current induced by superfusion with tetramethylammonium$^+$ ($TMA^+$) or 10 mM $choline^+$. We then washed the oocytes with Ori buffer, incubated them for 45 s with Ori buffer containing 50 $\mu$M $MTSET^+$, 50 $\mu$M $MTSET^+$ plus 10 mM $TMA^+$, or 50 $\mu$M $MTSET^+$ plus 10 mM $choline^+$. The oocytes were then washed again with Ori buffer, and the inward currents induced by 10 mM $TMA^+$ or $choline^+$ were measured (Fig. 10, *B* and *C*). The irreversible inhibition of cation-induced currents by $MTSET^+$ was significantly reduced when the incubation with $MTSET^+$ at −50 mV was performed in the presence of $TMA^+$ or $choline^+$ indicating substrate effects on the accessibility of Cys-478. The data therefore indicates movements of Gly-478 during transport.

## DISCUSSION

Employing fluorescence labeling of amino acids located at the extracellular plasma membrane surface of TMHs 5, 8, and 11 of rOct1, we observed membrane potential-dependent fluorescence changes indicating movements at these positions. The fluorescence changes at these indicator positions were blocked, blunted, or reversed in the presence of organic cation substrates or with a cationic nontransported inhibitor. The voltage-dependent fluorescence changes at the indicator positions in TMHs 5 and 11 were blocked when Gly-478 in TMH 11 was replaced by cysteine or serine, whereas modification of the replaced cysteine by $MTSET^+$ was required to block the fluorescence changes of TMH 8. Glycine 478 is located within the outward-open cleft one helix turn above aspartate 475, which interacts with $TEA^+$ during transport (14). Because rOct1 mediates membrane potential-dependent transport of organic cations implicating potential- and cation-dependent structural changes, the observed movements suggest that TMHs 5, 8, and 11 participate in the structural changes during transport. This interpretation is supported by the observation that capacitance changes of rOct1(10ΔC) and rOct1(10ΔC,G478C), which were induced by $TEA^+$ and $choline^+$, were abolished when transport was blocked by modification of Cys-478 with $MTSET^+$.

By TMRM attached to external parts of TMHs 5, 8, and 11, movements are indicated that are associated with mechanistically relevant structural changes during transport because they were blunted or abolished when transport was reduced or blocked by mutation or modification of Gly-478. However, the movements at the indicator positions may not be linked tightly to transport-related structural changes. This is probably true for the movements observed at the indicator positions in TMHs 5 and 8 because mutations and TMRM modification at these positions did not change Michaelis-Menten ($K_m$) values for $MPP^+$ nor the affinity for $TBuA^+$ (Table 1). At variance, the movements of amino acid 483 in TMH 11 appear to be directly linked to a transport-related structural change occurring after ligand binding because the exchange F483C decreased the $K_m$ values for $MPP^+$ by 50% and increased the affinity for $TBuA^+$ 10-fold (Table 1). A direct link of movements of Phe-483 to an initial structural change during transport is also supported by the observation that $choline^+$, $MPP^+$, and $TBuA^+$ exhibited

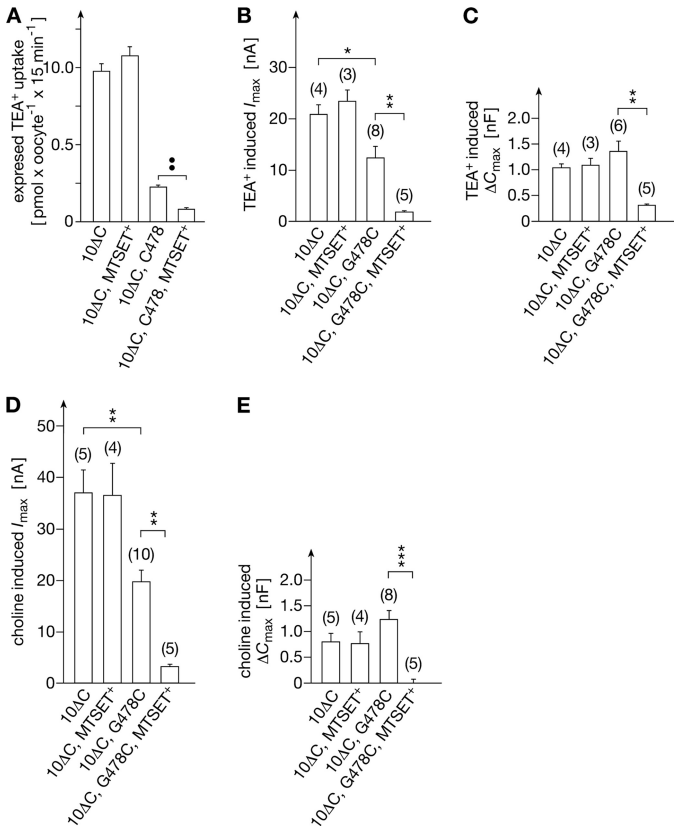


FIGURE 8. **Inhibition of organic cation transport and cation-induced capacitance changes by modification of rOct1(10ΔC,G478C) with MTSET$^+$.** rOct1(10ΔC) and rOct1(10ΔC, G478C) were expressed in oocytes. The oocytes were incubated for 10 min without or with 100 $\mu$M MTSET$^+$ and washed. Uptake of 9 $\mu$M [$^{14}$C]TEA$^+$ (*A*), currents induced by superfusion with 1 mM TEA$^+$ at −50 mV (*B*), or by superfusion with 10 mM choline$^+$ at −50 mV (*D*), and capacitance changes by 1 mM TEA$^+$ (*C*), or 10 mM choline$^+$ (*E*) were measured. Means ± S.E. are shown. *A,* uptake measured in transporter-expressing oocytes was corrected for nonspecific uptake in noninjected oocytes. 24–30 oocytes from three independent experiments are presented. The number of analyzed oocytes in *B–E* is indicated in *parentheses*. *, $p < 0.05$; **, $p < 0.01$; ***, $p < 0.001$.

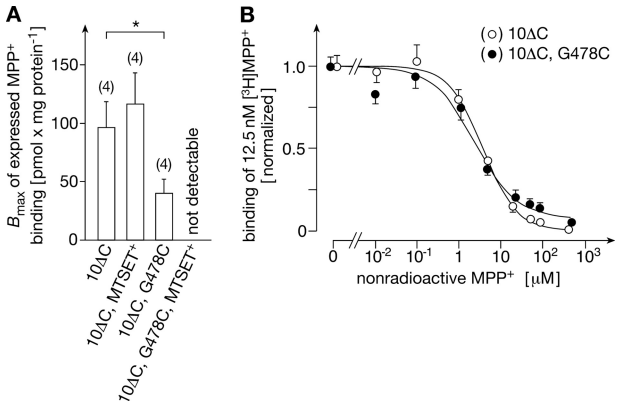


FIGURE 9. **Inhibition of MPP$^+$ binding by modification of rOct1(10ΔC,G478C) with MTSET$^+$.** HEK293 cells stably transfected with rOct1(10ΔC) or rOct1(10ΔC,G478C) were suspended, incubated for 1 min at 37 °C without and with 1 mM MTSET$^+$, washed, and cooled to 0 °C. Transporter expressed binding of 12.5 nM [$^3$H]MPP$^+$ that could be blocked by 5 mM nonradioactive MPP$^+$ was measured at 0 °C in the presence of various concentrations (0.001–100 $\mu$M) of nonradioactive MPP$^+$. *A,* maximally expressed MPP$^+$ binding calculated by fitting one-site binding kinetics to the data. Means ± S.E. and number of independent experiments are shown. In each experiment, four measurements per concentration of MPP$^+$ were performed. *, $p < 0.05$. *B,* comparison of the affinity of MPP$^+$ binding. The replacement of expressed binding of 12.5 nM [$^3$H]MPP$^+$ by nonradioactive MPP$^+$ is indicated. Means ± S.E. of four experiments are indicated. In each experiment, four measurements were performed per concentration of MPP$^+$.

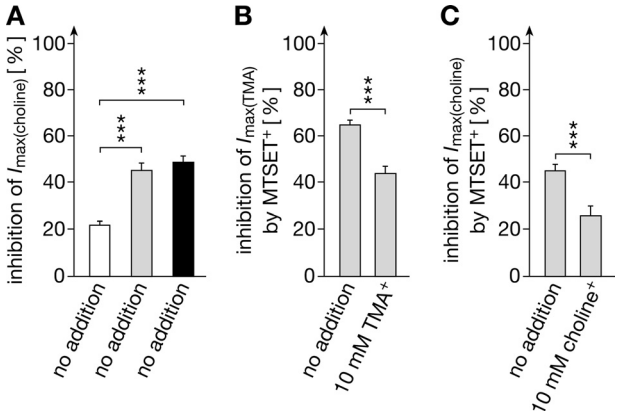


FIGURE 10. **Accessibility of cysteine 478 in rOct1(10ΔC,G478C) to modification by MTSET$^+$ is dependent on the membrane potential and on the presence of transported cations.** rOct1(10ΔC,G478C) was expressed in oocytes clamped to −50 mV, and the maximal currents induced by 10 mM choline ($I_{max(choline)}$) (*A* and *C*) or 10 mM tetramethylammonium$^+$ ($I_{max(TMA)}$) (*B*) were measured. After washing, oocytes were clamped to 0 mV (*open columns*), −50 mV (*gray columns*), or −100 mV (*black columns*), incubated for 45 s with Ori buffer containing 50 $\mu$M MTSET$^+$, washed, and clamped to −50 mV. Thereafter, the currents induced by superfusion with 10 mM choline$^+$ (*A* and *C*) or 10 mM TMA$^+$ (*B*) were measured again. Means ± S.E. of inhibition of currents induced by choline$^+$ or TMA$^+$ are presented. Numbers of analyzed oocytes are given in *parentheses*. ***, $p < 0.001$.

identical effects on the membrane potential-dependent structural changes (Fig. 2). In contrast, MPP$^+$ and TBuA$^+$ exhibited differential effects on fluorescence changes at the indicator positions in TMHs 5 and 8 (Fig. 2). This suggests a less tight and more indirect coupling to transport-related structural changes, which may allow varying allosteric effects of different ligands.

The observed effects of the mutations of Gly-478 and of the modification of cysteine in this position indicate a mechanistic role of TMH 11 for transport and suggest that Gly-478 is located in a domain, which is critically involved in structural changes during transport. The G478C mutation decreased the turnover for MPP$^+$ transport by about 40%, reversed the voltage-dependent fluorescence change at indicator position 483 in TMH 11, and increased the onset of the observed fluorescence change. Identical effects on the fluorescence were observed when glycine 478 was replaced by serine. The onset of the observed fluorescence changes within 100 ms and the increase of fluorescence onset seen for G478C, which was paralleled by a decrease of MPP$^+$ turnover, indicate that the observed structural fluorescence change is not time-limiting for translocation. In contrast to the mutations of Gly-478, the modification of Cys-478 by MTSET$^+$ abrogated the transition from the outward-open to the inward-open conformation because transport activity was blocked. The remaining 10% activity of MPP$^+$ transport after MTSET$^+$ modification is most probably due to activity of unmodified transporter molecules as the functional properties of the remaining activity were identical to transporter properties without MTSET$^+$ treatment. The observed membrane potential-dependent fluorescence change at indicator position 483 that was reversed after exchange of glycine 478 by cysteine or serine probably represents an initial structural change during transport following substrate binding. This

interpretation is supported by the observation that the fluorescence change was not only reversed by the transported cations $MPP^+$ and $choline^+$ but also by the nontransported inhibitor $TBuA^+$.

According to homology structure models of rOct1, the outward-open and inward-open clefts of rOct1 are formed by TMHs 1, 2, 4, 5, 7, 8, 10, and 11 (10, 13). Extensive mutagenesis data in rOct1 provided evidence that three amino acids in central parts of TMH 2 (Phe-160), TMH 4 (Trp-218), and TMH 11 (Asp-475) are directly involved in binding of organic cations during transport (4).[5] Mutations of several other amino acids that are located in more peripheral regions of TMH 4 (Y222F and T226A) and TMH 10 (R440K, L447Y, and Q448E) also led to changes in affinity and/or selectivity of substrates. It has not been clarified whether the observed effects of these mutations were due to direct or indirect effects on substrate binding, due to effects on high affinity binding sites that modulate transport (13, 32), or due to effects on transport-related structural changes, which alter transport kinetics.

The observed one-to-one coupling between translocated organic cations and translocated charges at negative membrane potential (9) in combination with the observation that outward-open and inward-open conformations of rOct1 models comprising several identical amino acids within their innermost parts of the clefts (4, 12) suggests that rOct1 undergoes an intermediate structural state in which the substrate is occluded and does not allow passage of small inorganic ions. In the structural models of the outward-open and inward-open conformations, cleft-forming TMHs 1, 2, 5, 7, 8, 10, and 11 are almost straight, whereas TMH 4 is bent (4, 9–11, 33). Interestingly, Trp-218 is located at the hinge angle of TMH 4 and occludes the transport path together with Phe-160 and Asp-475, which are located in the central parts of TMHs 2 and 11. OCTs seem not to contain discontinuous TMHs like various other ion membrane transporters (34) that enable different orientations of external and internal parts of TMHs during transport and do contain amino acids in the connecting loops involved in transport mechanism. Because it seems likely that differential movements of external and internal parts of TMHs also occur during transport by OCTs, we looked for conserved glycine residues in central parts of cleft-forming TMHs that may provide flexibility for such movements (16). TMH 7 contains one conserved central glycine residue, and TMH 4 has also one glycine that is conserved in most OCTs. This glycine is located before Trp-218, which is involved in substrate binding (35). TMHs 2, 5, 10, and 11 contain two conserved glycine residues in the center (35). Whereas the two glycine residues in TMHs 2, 5, and 10 are not consecutive, the two glycine residues in TMH 11 (Gly-477 and Gly-478) are juxtaposed. This allows high flexibilities of the external and internal parts of TMH 11 and supports our interpretation that Gly-478 is located within a substrate binding hinge domain allowing structural changes during transport. This hinge domain (supplemental Fig. 1) may contain Cys-474, Asp-475, Leu-476, Gly-477, and Gly-478 of rOct1. With the exception of Leu-476, these amino acids are conserved in OCT1–3 from different species but not in organic cation/zwitterion OCTN transporters and organic anion transporters of the SLC22 family. The proposed hinge domain appears to be critically involved in the transport mechanism. Previous mutagenesis studies indicated that Asp-475 binds $TEA^+$ and is critical for cation-specific turnover (4, 14). Recently Wright and co-workers (15) reported that the exchange of Cys-474 in hOCT2 by alanine increased the affinity for $TEA^+$. This suggests that Cys-474 also participates in $TEA^+$ binding. This study indicates that the accessibility of cysteine introduced at position 478 is reduced by substrates and altered by the membrane potential suggesting substrate-induced movements of Gly-478.

The proposed role of TMH 11 containing the above-described substrate binding hinge domain may help to understand how modifications of cysteine 451 at the intracellular loop between TMHs 10 and 11 and mutations of Cys-451 alter cation-induced currents and affinities of substrates (18). The model of the outward-open conformation of rOct1 predicts that Cys-451 is tightly packed against residues Trp-218 in TMH4, Leu-447 in TMH 10 and Leu-465, Val-469, and Ala-470 in TMH 11 and that replacement of Cys-451 by methionine as also done in rOct1(10ΔC) might alter the position of the internal part of TMH 11 (supplemental Fig. 11). This may change positioning of the functionally important hinge domain.

In summary, we identified a substrate binding domain in the middle of TMH 11, which is conserved in OCTs. This domain appears to be mechanistically important for a transport-related structural change that includes bending to TMH 11, which may be required for substrate occlusion. It appears to be pivotal for substrate translocation and could be a switch, which triggers substrate occlusion following substrate binding.

[5] S. Rehman, V. Gorboulev, and H. Koepsell, unpublished data.

## REFERENCES


1. Koepsell, H., Lips, K., and Volk, C. (2007) Polyspecific organic cation transporters. Structure, function, physiological roles, and biopharmaceutical implications. *Pharm. Res.* **24,** 1227–1251
2. Nies, A. T., Koepsell, H., Damme, K., and Schwab, M. (2011) Organic cation transporters (OCTs, MATEs), *in vitro* and *in vivo* evidence for the importance in drug therapy. *Handb. Exp. Pharmacol.* **201,** 105–167
3. Shu, Y., Sheardown, S. A., Brown, C., Owen, R. P., Zhang, S., Castro, R. A., Ianculescu, A. G., Yue, L., Lo, J. C., Burchard, E. G., Brett, C. M., and Giacomini, K. M. (2007) Effect of genetic variation in the organic cation transporter 1 (OCT1) on metformin action. *J. Clin. Invest.* **117,** 1422–1431
4. Koepsell, H. (2011) Substrate recognition and translocation by polyspecific organic cation transporters. *Biol. Chem.* **392,** 95–101
5. Kanner, B. I. (2005) Molecular physiology. Intimate contact enables transport. *Nature* **437,** 203–205
6. Rosental, N., and Kanner, B. I. (2010) A conserved methionine residue controls the substrate selectivity of a neuronal glutamate transporter. *J. Biol. Chem.* **285,** 21241–21248
7. Budiman, T., Bamberg, E., Koepsell, H., and Nagel, G. (2000) Mechanism of electrogenic cation transport by the cloned organic cation transporter 2 from rat. *J. Biol. Chem.* **275,** 29413–29420
8. Volk, C., Gorboulev, V., Budiman, T., Nagel, G., and Koepsell, H. (2003) Different affinities of inhibitors to the outwardly and inwardly directed substrate-binding site of organic cation transporter 2. *Mol. Pharmacol.* **64,** 1037–1047
9. Schmitt, B. M., Gorbunov, D., Schlachtbauer, P., Egenberger, B., Gorboulev, V., Wischmeyer, E., Müller, T., and Koepsell, H. (2009) Charge-to-substrate ratio during organic cation uptake by rat OCT2 is voltage-dependent and altered by exchange of glutamate 448 with glutamine. *Am. J. Physiol. Renal Physiol.* **296,** F709–F722

10. Popp, C., Gorboulev, V., Müller, T. D., Gorbunov, D., Shatskaya, N., and Koepsell, H. (2005) Amino acids critical for substrate affinity of rat organic cation transporter 1 line the substrate binding region in a model derived from the tertiary structure of lactose permease. *Mol. Pharmacol.* **67,** 1600–1611
11. Perry, J. L., Dembla-Rajpal, N., Hall, L. A., and Pritchard, J. B. (2006) A three-dimensional model of human organic anion transporter 1. Aromatic amino acids required for substrate transport. *J. Biol. Chem.* **281,** 38071–38079
12. Volk, C., Gorboulev, V., Kotzsch, A., Müller, T. D., and Koepsell, H. (2009) Five amino acids in the innermost cavity of the substrate binding cleft of organic cation transporter 1 interact with extracellular and intracellular corticosterone. *Mol. Pharmacol.* **76,** 275–289
13. Gorbunov, D., Gorboulev, V., Shatskaya, N., Mueller, T., Bamberg, E., Friedrich, T., and Koepsell, H. (2008) High affinity cation binding to organic cation transporter 1 induces movement of helix 11 and blocks transport after mutations in a modeled interaction domain between two helices. *Mol. Pharmacol.* **73,** 50–61
14. Gorboulev, V., Volk, C., Arndt, P., Akhoundova, A., and Koepsell, H. (1999) Selectivity of the polyspecific cation transporter rOCT1 is changed by mutation of aspartate 475 to glutamate. *Mol. Pharmacol.* **56,** 1254–1261
15. Pelis, R. M., Dangprapai, Y., Cheng, Y., Zhang, X., Terpstra, J., and Wright, S. H. (2012) Functional significance of conserved cysteines in the human organic cation transporter 2. *Am. J. Physiol. Renal Physiol.* **303,** F313–F320
16. Pace, C. N., and Scholtz, J. M. (1998) A helix propensity scale based on experimental studies of peptides and proteins. *Biophys. J.* **75,** 422–427
17. Veyhl, M., Spangenberg, J., Püschel, B., Poppe, R., Dekel, C., Fritzsch, G., Haase, W., and Koepsell, H. (1993) Cloning of a membrane-associated protein that modifies activity and properties of the $Na^+$-D-glucose cotransporter. *J. Biol. Chem.* **268,** 25041–25053
18. Sturm, A., Gorboulev, V., Gorbunov, D., Keller, T., Volk, C., Schmitt, B. M., Schlachtbauer, P., Ciarimboli, G., and Koepsell, H. (2007) Identification of cysteines in rat organic cation transporters rOCT1 (C322, C451) and rOCT2 (C451) critical for transport activity and substrate affinity. *Am. J. Physiol. Renal Physiol.* **293,** F767–F779
19. Ho, S. N., Hunt, H. D., Horton, R. M., Pullen, J. K., and Pease, L. R. (1989) Site-directed mutagenesis by overlap extension using the polymerase chain reaction. *Gene* **77,** 51–59
20. Keller, T., Egenberger, B., Gorboulev, V., Bernhard, F., Uzelac, Z., Gorbunov, D., Wirth, C., Koppatz, S., Dötsch, V., Hunte, C., Sitte, H. H., and Koepsell, H. (2011) The large extracellular loop of organic cation transporter 1 influences substrate affinity and is pivotal for oligomerization. *J. Biol. Chem.* **286,** 37874–37886
21. Busch, A. E., Quester, S., Ulzheimer, J. C., Waldegger, S., Gorboulev, V., Arndt, P., Lang, F., and Koepsell, H. (1996) Electrogenic properties and substrate specificity of the polyspecific rat cation transporter rOCT1. *J. Biol. Chem.* **271,** 32599–32604
22. Gründemann, D., and Koepsell, H. (1994) Ethidium bromide staining during denaturation with glyoxal for sensitive detection of RNA in agarose gel electrophoresis. *Anal. Biochem.* **216,** 459–461
23. Busch, A. E., Karbach, U., Miska, D., Gorboulev, V., Akhoundova, A., Volk, C., Arndt, P., Ulzheimer, J. C., Sonders, M. S., Baumann, C., Waldegger, S., Lang, F., and Koepsell, H. (1998) Human neurons express the polyspecific cation transporter hOCT2, which translocates monoamine neurotransmitters, amantadine, and memantine. *Mol. Pharmacol.* **54,** 342–352
24. Geibel, S., Zimmermann, D., Zifarelli, G., Becker, A., Koenderink, J. B., Hu, Y. K., Kaplan, J. H., Friedrich, T., and Bamberg, E. (2003) Conformational dynamics of $Na^+/K^+$- and $H^+/K^+$-ATPase probed by voltage clamp fluorometry. *Ann. N.Y. Acad. Sci.* **986,** 31–38
25. Schmitt, B. M., and Koepsell, H. (2002) An improved method for real-time monitoring of membrane capacitance in *Xenopus laevis* oocytes. *Biophys. J.* **82,** 1345–1357
26. Schmitt, B. M., and Koepsell, H. (2005) Alkali cation binding and permeation in the rat organic cation transporter rOCT2. *J. Biol. Chem.* **280,** 24481–24490
27. Kamsteeg, E. J., and Deen, P. M. (2001) Detection of aquaporin-2 in the plasma membranes of oocytes. A novel isolation method with improved yield and purity. *Biochem. Biophys. Res. Commun.* **282,** 683–690
28. Vernaleken, A., Veyhl, M., Gorboulev, V., Kottra, G., Palm, D., Burckhardt, B. C., Burckhardt, G., Pipkorn, R., Beier, N., van Amsterdam, C., and Koepsell, H. (2007) Tripeptides of RS1 (RSC1A1) inhibit a monosaccharide-dependent exocytotic pathway of $Na^+$-D-glucose cotransporter SGLT1 with high affinity. *J. Biol. Chem.* **282,** 28501–28513
29. Valentin, M., Kühlkamp, T., Wagner, K., Krohne, G., Arndt, P., Baumgarten, K., Weber, W., Segal, A., Veyhl, M., and Koepsell, H. (2000) The transport modifier RS1 is localized at the inner side of the plasma membrane and changes membrane capacitance. *Biochim. Biophys. Acta* **1468,** 367–380
30. Keller, T., Schwarz, D., Bernhard, F., Dötsch, V., Hunte, C., Gorboulev, V., and Koepsell, H. (2008) Cell-free expression and functional reconstitution of eukaryotic drug transporters. *Biochemistry* **47,** 4552–4564
31. Ciarimboli, G., Koepsell, H., Iordanova, M., Gorboulev, V., Dürner, B., Lang, D., Edemir, B., Schröter, R., Van Le, T., and Schlatter, E. (2005) Individual PKC phosphorylation sites in organic cation transporter 1 determine substrate selectivity and transport regulation. *J. Am. Soc. Nephrol.* **16,** 1562–1570
32. Minuesa, G., Volk, C., Molina-Arcas, M., Gorboulev, V., Erkizia, I., Arndt, P., Clotet, B., Pastor-Anglada, M., Koepsell, H., and Martinez-Picado, J. (2009) Transport of lamivudine [(−)-$\beta$-L-2′,3′-dideoxy-3′-thiacytidine] and high affinity interaction of nucleoside reverse transcriptase inhibitors with human organic cation transporters 1, 2, and 3. *J. Pharmacol. Exp. Ther.* **329,** 252–261
33. Zhang, X., Shirahatti, N. V., Mahadevan, D., and Wright, S. H. (2005) A conserved glutamate residue in transmembrane helix 10 influences substrate specificity of rabbit OCT2 (SLC22A2). *J. Biol. Chem.* **280,** 34813–34822
34. Screpanti, E., and Hunte, C. (2007) Discontinuous membrane helices in transport proteins and their correlation with function. *J. Struct. Biol.* **159,** 261–267
35. Koepsell, H., Gorboulev, V., and Arndt, P. (1999) Molecular pharmacology of organic cation transporters in kidney. *J. Membr. Biol.* **167,** 103–117